

STATISTICAL PROPERTIES OF SPARSE GAUSSIAN RANDOM SYMMETRICAL ENSEMBLE

M.M. DURAS, K. SOKALSKI AND P. SUŁKOWSKI

Institute of Physics, Jagellonian University
Reymonta 4, 30-059 Krakow, Poland
e-mail: piotr@izis.if.uj.edu.pl

(Received June 12, 1996; revised version received November 13, 1996)

Sparse Gaussian Random Symmetrical Ensemble has been introduced. Its statistical properties have been investigated. Transition from chaotic sub-ensemble to integrable one versus fraction of the matrix elements not equal to zero has been found. Jump of cumulative distribution function at energy $E = 0$ has been interpreted as an order parameter which differentiates between chaotic and integrable ensembles.

PACS numbers: 05.30. Ch, 02.10. Sp, 05.45. +b, 05.70. Fh

1. Introduction

Most models of solid state physics take into account a finite number of interaction zones. This is the reason for growing interest in the statistical properties of random bounded matrices [1]. There are systems, for instance: spin glasses, diluted spin systems [2], disordered conductors [3] and quantum percolation models [4], corresponding to models with randomly distributed interactions for which the number of interacting atoms with the fixed one is much less than the total number of atoms of that system. These simplifications of reality lead to the Schrödinger's equations represented by sparse Hermitian matrices. Also the quantum mechanical aspect of chaos should be mentioned as an example in this respect [5]. Considerations of general properties of the matrix ensembles having given dimension and symmetry lead to the problem of the statistical properties of the random matrices. The above approach suggests to investigate the statistical properties of the Sparse Random Matrix Ensemble — SRME [6–9]. Going to the sparse random matrix ensemble by diluting the \mathcal{N} -dimensional Gaussian orthogonal ensemble $\text{GOE}(\mathcal{N})$ one obtains the $\text{SRME}(p, \mathcal{N})$ which is characterized by a finite mean number p of randomly placed nonzero elements per matrix row

[8, 9]. A simpler ensemble than SRME, the $\mathcal{N} \times \mathcal{N}$ ($\mathcal{N} \rightarrow \infty$) real symmetric random matrices with elements $0, \pm 1$ and with mean number p of nonzero elements per row, has been studied in [10]. The density of states (DOS) ρ for such an ensemble was investigated by means of replica trick, and the integral equation was derived (compare equation (18) in [10]) giving the possibility of calculating density of states. Iteration of this integral equation gave a perturbative expansion of the density of states in powers of $1/p$, with leading term reproducing Wigner's semicircular law for $p \rightarrow \infty$ (compare equation (30) in [10]). For finite p , the leading nonperturbative contribution to the density of states was computed via the saddle point method. The density of states covers the entire interval $(-\infty, \infty)$ and it has tails extending beyond the semicircle $\rho(\mu) = (\frac{ep}{\mu^2})^{\mu^2}$, for $\mu \rightarrow \infty$. The statistical properties of sparse random matrices ensembles were investigated by means of supersymmetric approach [7]. The studied matrix is real, symmetric $\mathcal{N} \times \mathcal{N}$ ($\mathcal{N} \rightarrow \infty$), whose elements are independent, identically distributed random variables with certain probability distribution function $f(z) = (1-a)\delta(z) + ah(z)$, $0 \leq a \leq 1$, h has no δ singularity at $z = 0$, $a \int h(z)z^2 dz \sim \mathcal{N}^{-1}$. The supersymmetric approach was found to be equivalent to the replica trick method. In [1] Wigner random banded matrices with sparse structure were studied with given band parameter and sparsity. The mean value of the diagonal matrix elements is linearly increasing and the mean value of the off-diagonal elements is zero (compare equation (4) in [1]). The local density of states LDOS (or the strength function) instead of density of states was investigated. The integral equation for the local density of states was obtained (compare equation (5) in [1]). The numerical computation showing the transition between semicircle regime and Breit Wigner regime was done. We extend the work in [1, 7, 10] by defining the new SGRSE(x, \mathcal{N}). In our approach we characterize diluted GOE(\mathcal{N}) by fraction x of matrix elements not equal to zero. The $x\mathcal{N}^2$ matrix elements are zero-centred Gaussian distributed with variance equal to σ^2 , while the remaining elements are equal identically to zero, distributed everywhere randomly (including the diagonal). The elements are independent random variables.

In order to characterize the properties of investigated ensemble we calculate the distributions of finite elements instead of the density of states or local density of states which is a new approach.

Each pair of two numbers (x, \mathcal{N}) , where $0 \leq x \leq 1$ and \mathcal{N} is a natural number, corresponds to an ensemble. Thus variation of x leads to a continuum of \mathcal{N} dimensional ensembles. The matrix elements equal to zero are constant random variables, thus SGRSE(x, \mathcal{N}) is an extension of the GOE(\mathcal{N}) and SGRSE($1, \mathcal{N}$)=GOE(\mathcal{N}). In this paper we investigate the universal properties of SGRSE(x, \mathcal{N}). On the base of the numerical calculations for SGRSE(x, \mathcal{N}) and their comparison to the analytic exact results

for GOE(2) and GOE(3) we show a continuous transition from the ensembles possessing sparse matrix properties to the ensembles possessing dense matrix properties. The transition occurs at x_c . Then we show how well the statistical properties of the SGRSE(x, \mathcal{N}) are approximated by the GOE(2) and GOE(3) properties, for $x > x_c$. There is a number of statistical properties of the eigenvalues of random matrices which are used in analysis of the spectral properties of systems. For the purpose of this paper we select the following statistical characters: *i*) the nearest neighbor spacing distribution [11–14], *ii*) the second difference distribution [15], *iii*) the three point first finite elements distributions [15].

The aim of this paper is to investigate statistical properties of SGRSE(x, \mathcal{N}) by numerical simulations and their comparison to the theoretical results for the distributions of the above finite elements.

The paper is organized as follows: Section 2 provides the distribution of the spacing, asymmetrical three point first finite element, symmetrical three point first finite element, and second difference for the GOE and for the three level quantum integrable system (Poisson ensemble). Section 3 presents results of numerical calculations and their comparison to the analytical distributions. Section 4 discusses the obtained results.

2. The distributions of the finite elements for the GOE and Poisson ensemble

In this section we approach four statistical characteristics used to investigate the problem defined in the Introduction.

The basic quantity of investigations in quantum chaos in many level system is the nearest neighbor spacing, that is the first difference between the two adjacent levels E_i, E_{i+1} . The i^{th} spacing s_i reads

$$s_i = \Delta^1 E_i = E_{i+1} - E_i. \quad (1)$$

It is seen from structure of spacing that s_i is a local quantity and it can describe neither homogeneity of level distribution nor the correlation between non-adjacent levels. The information about the nonlocal properties of the level system are built into the distributions of the higher order finite elements. In order to complete statistical description of the quantum level system we have derived analytic formulas for the distributions of some higher finite elements [15]. We studied the i^{th} second difference of the three adjacent energy levels E_i, E_{i+1}, E_{i+2} in the level system defined as follows:

$$\Delta^2 E_i = \Delta^1 E_{i+1} - \Delta^1 E_i = E_i + E_{i+2} - 2E_{i+1}. \quad (2)$$

The probability density function of the second difference was computed analytically for the following ensembles GOE(3) as well as for the quantum

integrable three level system. This probability density function was proved to describe the tendency of the both chaotic and integrable system towards homogeneity of the level distribution. Moreover, we also studied a series of experimental nuclear spectra, and we observed that the levels of these spectra also tend to be distributed homogeneously. We also studied the three energy level quantum system and we derived the probability density functions of the three point finite elements of energy levels for the GOE(3) and for the quantum integrable system. We studied the following three point finite elements:

$$\Delta_{a,\text{fin}}^1 E_i = \frac{1}{2(i+1-i)}(-3E_i + 4E_{i+1} - E_{i+2}), \quad (3)$$

(see [16], we named $\Delta_{a,\text{fin}}^1 E_i$ the i^{th} asymmetrical three point first finite element) and

$$\Delta_{s,\text{fin}}^1 E_{i+1} = \frac{1}{2(i+1-i)}(E_{i+2} - E_i), \quad (4)$$

(see [16], we called $\Delta_{s,\text{fin}}^1 E_{i+1}$ the i^{th} symmetrical three point first finite element). We derived analytically the probability density functions of these finite elements for the GOE(3) as well as for the sequence of the three adjacent randomly distributed energy levels. The distribution of the quantity named first order spacing (or the next-nearest neighbor spacing) for the ordered sequence of the levels randomly distributed is given in [17], formula (3). The explicit formulas for its distributions were derived in [18], formula (6) for the GOE(3) and in [19], formula (89) for the three-dimensional Gaussian unitary ensemble GUE(3). The distributions of the symmetrical three point first finite element and of the first order spacing are consistent with each other. The analytic formulas for the above distributions for the GOE(3) and for the integrable system are given below.

In order to compare the analytical distributions with their numerical simulations we divide the above mentioned four quantities by mean spacing, making them dimensionless.

We assume the GOE(2). The mean spacing for the GOE(2) reads (compare [20], formula (6.6.10)):

$$\overline{S^{\text{GOE}(2)}} = \sqrt{2\pi} \sigma, \quad (5)$$

where σ^2 is the variance of the off-diagonal elements of the GOE(2) matrix. We make the spacing dimensionless by dividing it by the mean spacing $\overline{S^{\text{GOE}(2)}}$:

$$T^{\text{GOE}(2)} = s_1 / \overline{S^{\text{GOE}(2)}}. \quad (6)$$

The probability density function of $T^{\text{GOE}(2)}$ is (compare [20], formula (6.6.11)):

$$f_{T^{\text{GOE}(2)}}(x) = \Theta(x) \frac{\pi}{2} x \exp\left(-\frac{\pi x^2}{4}\right), \quad (7)$$

where Θ is Heaviside function:

$$\Theta(x) = \begin{cases} 1 & \text{for } x \geq 0 \\ 0 & \text{for } x < 0. \end{cases}$$

Now, we assume the $\text{GOE}(3)$. The mean spacing for the $\text{GOE}(3)$ reads (compare [18], formula (5)):

$$\overline{S^{\text{GOE}(3)}} = \frac{3\sqrt{3}\sigma}{\sqrt{2\pi}}, \quad (8)$$

where σ^2 is the variance of the off-diagonal elements of the $\text{GOE}(3)$ matrix.

We make the asymmetrical three point finite element dimensionless by dividing it by the mean spacing $\overline{S^{\text{GOE}(3)}}$:

$$X^{\text{GOE}(3)} = \Delta_{a,\text{fin}}^1 E_1 / \overline{S^{\text{GOE}(3)}}. \quad (9)$$

The probability density function of $X^{\text{GOE}(3)}$ reads [15]:

$$\begin{aligned} f_{X^{\text{GOE}(3)}}(x) = & \frac{81}{228488\pi^2} (910\sqrt{13}\pi x - 315\sqrt{13}x^3 \\ & + (1638x^2 + 2704\pi) \exp(-\frac{25x^2}{52\pi}) \\ & + \sqrt{13}x(315x^2 - 910\pi) \operatorname{erf}(\frac{5x}{2\sqrt{13}\pi})) \exp(-\frac{27x^2}{52\pi}) \quad \text{for } x \geq 0, \end{aligned} \quad (10)$$

$$\begin{aligned} f_{X^{\text{GOE}(3)}}(x) = & -\frac{81}{228488\pi^2} (-910\sqrt{13}\pi x + 315\sqrt{13}x^3 \\ & + (390x^2 - 2704\pi) \exp(-\frac{441x^2}{52\pi}) \\ & + \sqrt{13}x(315x^2 - 910\pi) \operatorname{erf}(\frac{21x}{2\sqrt{13}\pi})) \exp(-\frac{27x^2}{52\pi}) \quad \text{for } x < 0, \end{aligned}$$

where the error function is

$$\operatorname{erf}(x) = \frac{2}{\sqrt{\pi}} \int_0^x dt \exp(-t^2).$$

We make the symmetrical three point finite element dimensionless by defining the following dimensionless random variable for the GOE(3)

$$Y^{\text{GOE}(3)} = \Delta_{s,\text{fin}}^1 E_2 / \overline{S^{\text{GOE}(3)}}. \quad (11)$$

The probability density function of $Y^{\text{GOE}(3)}$ is [15]:

$$\begin{aligned} f_{Y^{\text{GOE}(3)}}(x) = & \frac{81x}{4\pi^2} \left(6x \exp\left(-\frac{9x^2}{\pi}\right) \right. \\ & \left. + (9x^2 - 2\pi) \exp\left(-\frac{27x^2}{4\pi}\right) \operatorname{erf}\left(\frac{3x}{2\sqrt{\pi}}\right) \right). \end{aligned} \quad (12)$$

Note, that the statistics of spacing between every second eigenvalue $Y^{\text{GOE}(\mathcal{N})}$ is exactly the same as the statistics of nearest neighbour spacing for Gaussian symplectic ensemble GSE, specially in the limit of large matrices $\mathcal{N} \rightarrow \infty$ [21].

In order to make the second difference dimensionless we divide it by the mean spacing $\overline{S^{\text{GOE}(3)}}$ and we define the new dimensionless random variable for the GOE(3)

$$Z^{\text{GOE}(3)} = \Delta^2 E_1 / \overline{S^{\text{GOE}(3)}}. \quad (13)$$

The probability density function of $Z^{\text{GOE}(3)}$ reads [15]:

$$f_{Z^{\text{GOE}(3)}}(x) = \frac{3}{2\pi} \exp\left(-\frac{9x^2}{4\pi}\right). \quad (14)$$

We assume now the quantum integrable system. The mean spacing throughout the level sequence is equal to D [17]. We make the spacing dimensionless by dividing it by the mean spacing D . We define the new dimensionless spacing for the quantum integrable system

$$T^{\text{I}} = \frac{s_1}{D}. \quad (15)$$

The probability density function of T^{I} is (compare [17], formula (3)):

$$f_{T^{\text{I}}}(x) = \Theta(x) \exp(-x). \quad (16)$$

We make the asymmetrical three point first finite element dimensionless by dividing it by the mean spacing D . We define the new dimensionless random variable for the quantum integrable system

$$X^{\text{I}} = \frac{\Delta_{a,\text{fin}}^1 E_1}{D}. \quad (17)$$

The probability density function of X^I is [15]:

$$f_{X^I}(x) = \begin{cases} \frac{1}{2} \exp(-\frac{2x}{3}) & \text{for } x \geq 0 \\ \frac{1}{2} \exp(2x) & \text{for } x < 0 \end{cases}. \quad (18)$$

We make the symmetrical three point finite element dimensionless by defining the following dimensionless random variable for the quantum integrable system

$$Y^I = \frac{\Delta_{s,\text{fin}}^1 E_1}{D}. \quad (19)$$

The probability density function of Y^I reads [15]

$$f_{Y^I}(x) = \Theta(x) 4x \exp(-2x). \quad (20)$$

In order to make the second difference dimensionless we divide it by the mean spacing D and we define the new dimensionless random variable for the quantum integrable system

$$Z^I = \frac{\Delta^2 E_1}{D}. \quad (21)$$

The probability density function of Z^I is [15]

$$f_{Z^I}(x) = \frac{1}{2} \exp(-|x|). \quad (22)$$

3. Simulations of the distributions of the finite elements for the sparse Gaussian real symmetrical random matrix ensemble

We generate a symmetrical matrix of a given dimension and density, nonzero elements of which are Gaussian distributed (procedure SPRANDSYM of package MATLAB, version 4.2c). We diagonalize this matrix with procedure EIG. The cumulative distribution function $N(E)$ that represents the spectra of the matrix 2000×2000 for the densities $x=0.0005, 0.05$ is plotted in Fig. 1a, and Fig. 1b, respectively. Near a certain value $x = x_c$ there is a change of character of function $N(E)$ (for instance for $\mathcal{N} = 400, x_c = 0.0135$). For $x < x_c$, $N(E)$ is a discontinuous function at the point $E = 0$. For the growing x the jump of function $\Delta N(0) = N(+0) - N(-0)$ is continuously decreasing to zero at x_c . On this basis one may say, that the matrix ensembles for $x < x_c$ differ qualitatively from the matrix ensembles for $x > x_c$. The observed effect may be interpreted as phase transition in the matrix ensemble $\text{SGRSE}(x, \mathcal{N})$. ΔN is an order parameter. The value of

x_c is a function of matrix dimension. It seems that there exist two different types of $\text{SGRSE}(x, \mathcal{N})$: for $x < x_c$ and for $x > x_c$. The critical value x_c is defined by the following limit:

$$\lim_{x \rightarrow x_c - 0} \Delta N = 0. \quad (23)$$

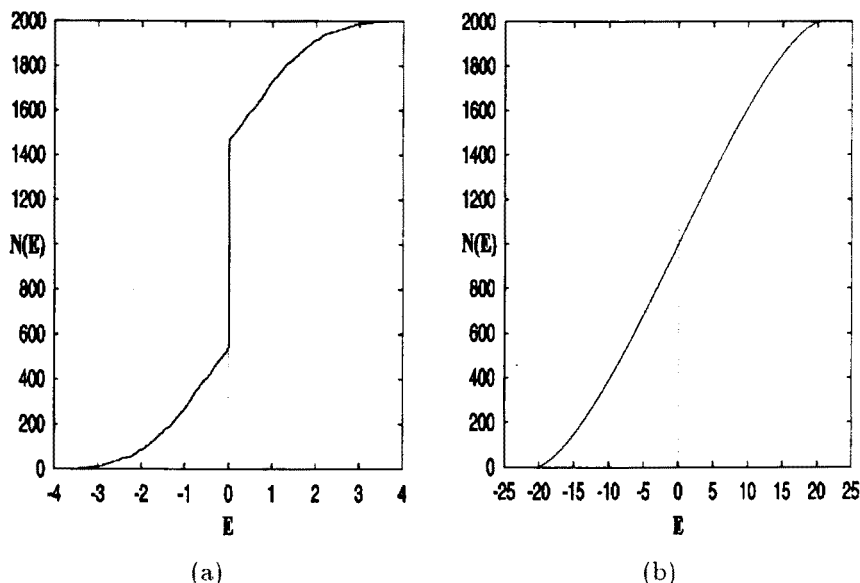


Fig. 1. (a) — The cumulative distribution function $N(E)$ for $x = 0.0005$, $\mathcal{N} = 2000$. (b) — The cumulative distribution function $N(E)$ for $x = 0.05$, $\mathcal{N} = 2000$.

The question what are statistical properties of these two sub-ensembles is natural in this place. Thus we calculate statistical measures described in Section 2 for both regions of x . Results for the region $x > x_c$ represented by $x = 0.05$ and $\mathcal{N} = 2000$ are presented in the Figs 2a–d. Results for $x < x_c$ represented by $x = 0.0005$ and $\mathcal{N} = 2000$ and by $x = 0.001$ and $\mathcal{N} = 2000$ are presented in the Figs 3a–d and Figs 4a–d, respectively.

All statistical measures have been collected from 50 random matrices, therefore each statistics is calculated from around 10^5 levels. Figures labeled by a, b, c, d present the distributions of the following finite elements: spacing s_i , asymmetrical three point first finite element $\Delta_{a,\text{fin}}^1 E_i$, symmetrical three point first finite element $\Delta_{s,\text{fin}}^1 E_{i+1}$ and second difference $\Delta^2 E_i$, respectively. Histograms represent the computer simulations, the solid lines and dashed ones correspond to the theoretical results for GOE and for integrable system, respectively. It is evident that for $x > x_c$ the theoretical results of GOE fit much better histograms than the theoretical results of the integrable system

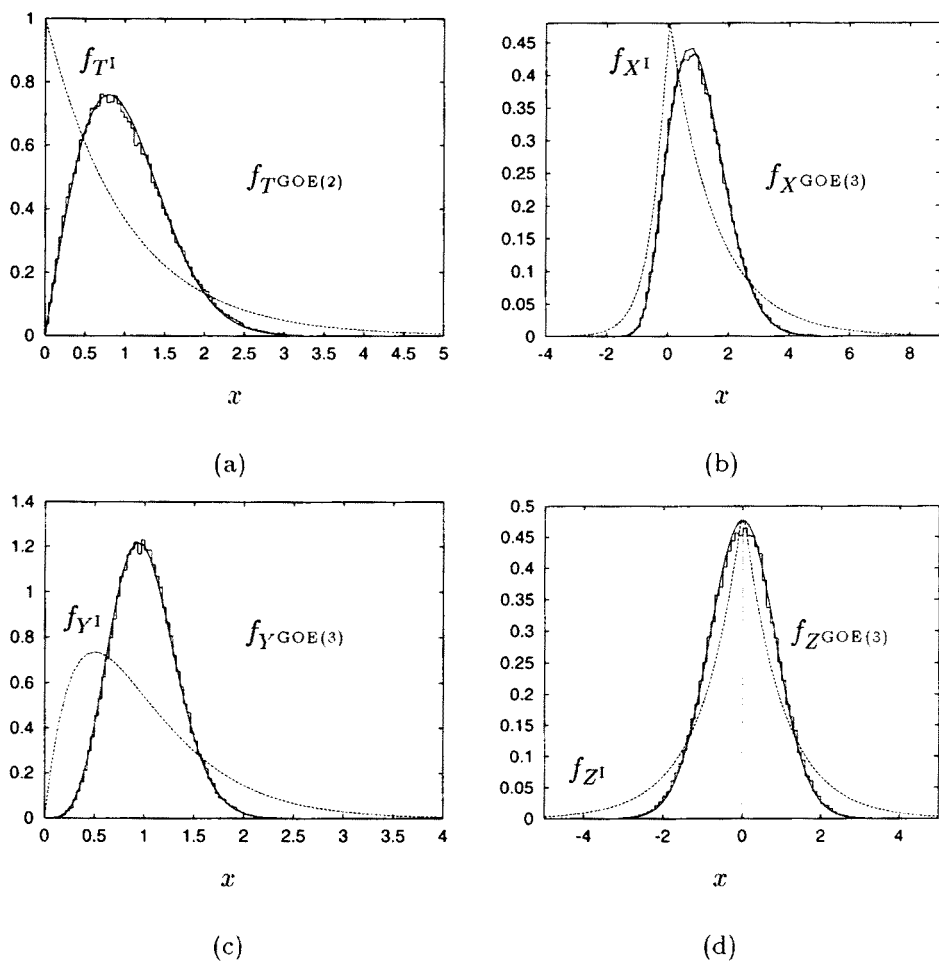


Fig. 2. (a) — The probability density function of the dimensionless spacing for the GOE(2) (solid line), for the integrable system (dashed line) and for $x = 0.05$ (histogram). (b) — The probability density function of the dimensionless asymmetrical three point first finite element for the GOE(3) (solid line), for the integrable system (dashed line) and for $x = 0.05$ (histogram). (c) — The probability density function of the dimensionless symmetrical three point first finite element for the GOE(3) (solid line), for the integrable system (dashed line) and for $x = 0.05$ (histogram). (d) — The probability density function of the dimensionless second difference for the GOE(3) (solid line), for the integrable system (dashed line) and for $x = 0.05$ (histogram).

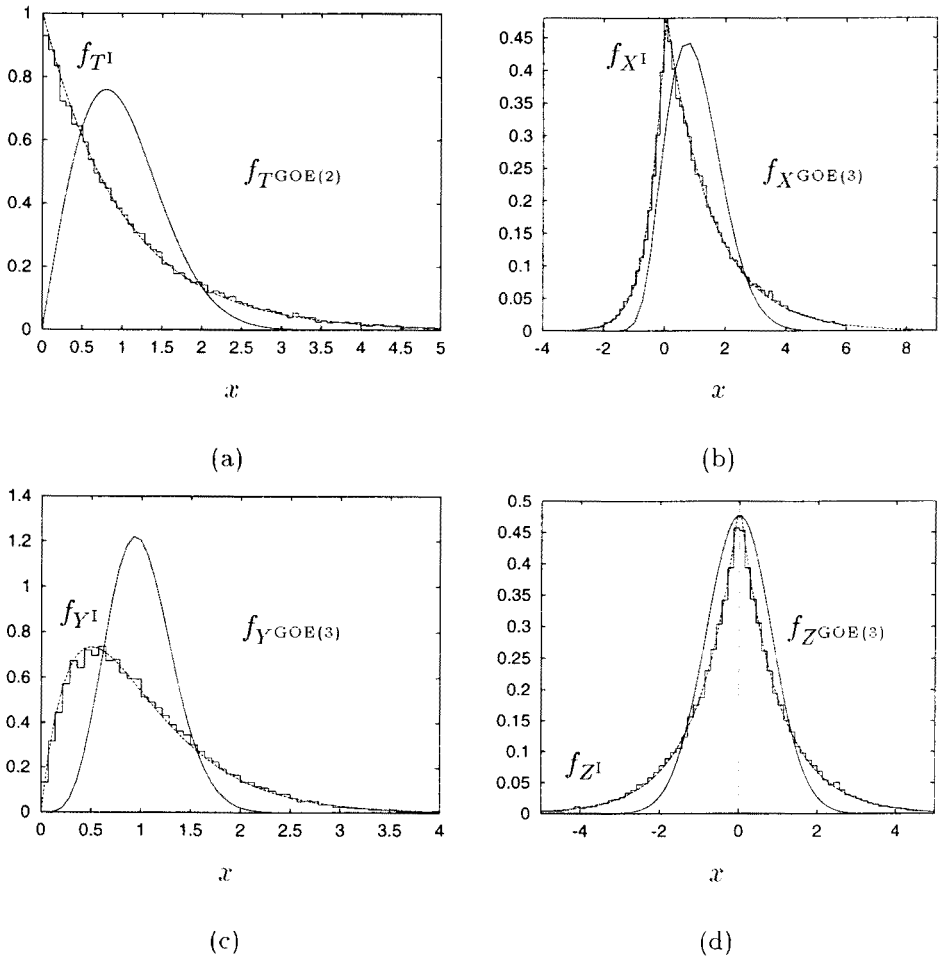


Fig. 3. (a) — The probability density function of the dimensionless spacing for the GOE(2) (solid line), for the integrable system (dashed line) and for $x = 0.0005$ (histogram). (b) — The probability density function of the dimensionless asymmetrical three point first finite element for the GOE(3) (solid line), for the integrable system (dashed line) and for $x = 0.0005$ (histogram). (3c) — The probability density function of the dimensionless symmetrical three point first finite element for the GOE(3) (solid line), for the integrable system (dashed line) and for $x = 0.0005$ (histogram). (d) — The probability density function of the dimensionless second difference for the GOE(3) (solid line), for the integrable system (dashed line) and for $x = 0.0005$ (histogram).

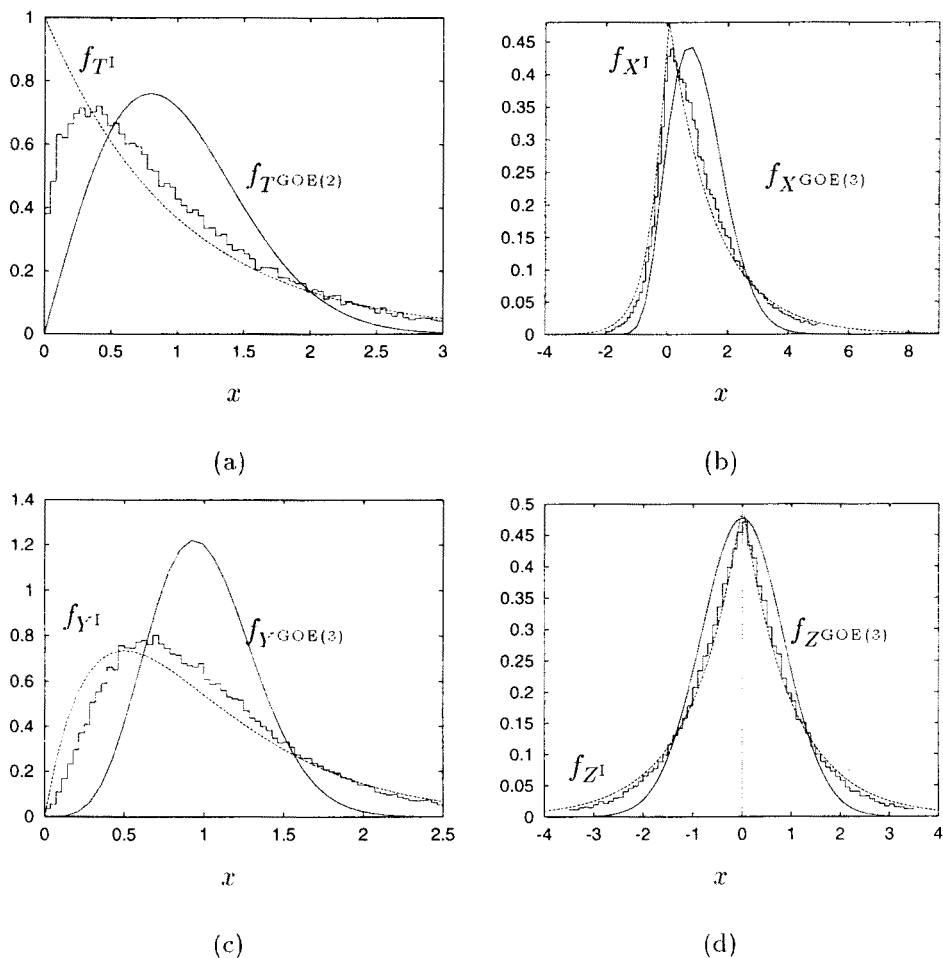


Fig. 4. (a) — The probability density function of the dimensionless spacing for the GOE(2) (solid line), for the integrable system (dashed line) and for $x = 0.001$ (histogram). (b) — The probability density function of the dimensionless asymmetrical three point first finite element for the GOE(3) (solid line), for the integrable system (dashed line) and for $x = 0.001$ (histogram). (c) — The probability density function of the dimensionless symmetrical three point first finite element for the GOE(3) (solid line), for the integrable system (dashed line) and for $x = 0.001$ (histogram). (d) — The probability density function of the dimensionless second difference for the GOE(3) (solid line), for the integrable system (dashed line) and for $x = 0.001$ (histogram).

do. Whereas, for $x < x_c$ the situation is opposite. The results of the integrable system fit the histograms while the GOE ones do not.

Comparing results presented in Figs 3(a)–(d) and Figs 4(a)–(d) one can see that the histograms fit better the theoretical results for integrable systems while the density x decreases, *e.g.* when the order parameter ΔN increases. This result shows that the system with high value of the order parameter is “more integrable” than the system having a lower value of ΔN . It has been shown elsewhere that the order parameter ΔN is a measure of number of independent invariants [22]. When the number of invariants is equal to \mathcal{N} then $\Delta N = 1$. Therefore, the order parameter is a measure of integrability, *e.g.* it measures how far the system is from the full integrability ($\Delta N = 1$).

Some statistical measures like $f_{X^{\text{GOE}(3)}}$ and $f_{Z^{\text{GOE}(3)}}$ get agreement with the theoretical results much faster than others: $f_{T^{\text{GOE}(2)}}$, $f_{Y^{\text{GOE}(3)}}$. This effect suggests that distributions of three point finite elements are more suitable for description of the integrable system than the distribution of spacing is.

On the base of presented results one can formulate the following hypothesis:

- $\text{SGRSE}(x < x_c(\mathcal{N}), \mathcal{N})$ is equivalent to the integrable system
- $\text{SGRSE}(x > x_c(\mathcal{N}), \mathcal{N})$ is equivalent to $\text{GOE}(\mathcal{N})$.

4. Conclusions

The results presented in Section 3 indicate a smooth phase transition from the chaotic systems to the integrable ones as a function of the density parameter x . It is convenient to describe such a phenomenon by quantities characteristic for phase transitions, like an order parameter and a phase diagram. Figs 1(a), (b) suggest that $\Delta N = N(+0) - N(-0)$ can play the role of the order parameter. An example of dependence of ΔN versus $\log(x)$ for dimension $\mathcal{N} = 100$ is presented in Fig. 5, where the log means decimal logarithm. This dependence is typical for the continuous phase transitions of the order higher than two.

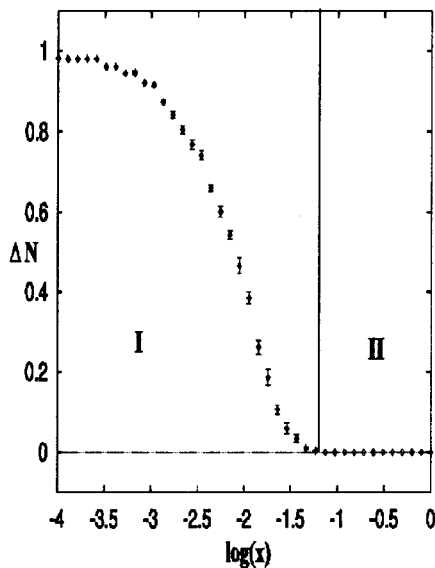


Fig. 5. The order parameter ΔN as a function of logarithm of density x for $\mathcal{N} = 100$ together with the errors.

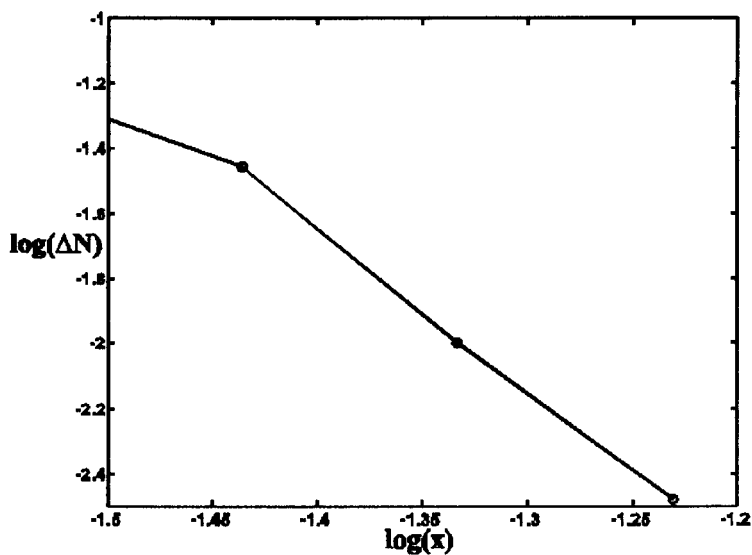


Fig. 6. The logarithm of the order parameter ΔN as a function of logarithms of density x for $\mathcal{N} = 100$ near the critical value x_c .

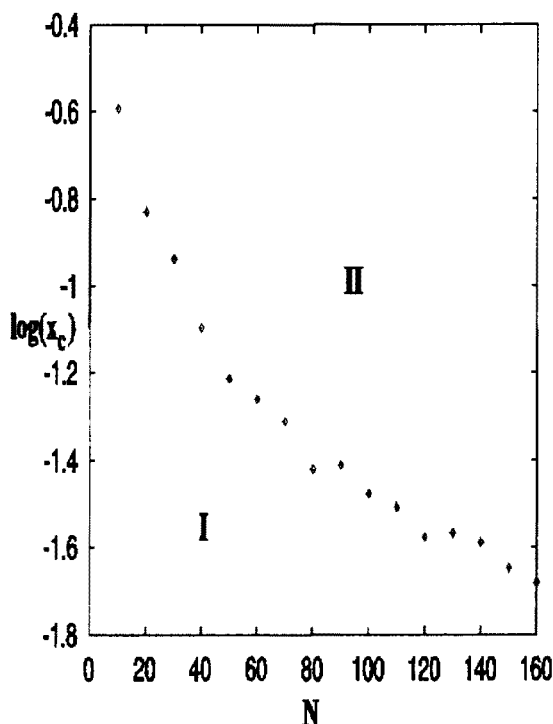


Fig. 7. The logarithm of the critical density x_c as a function of ensemble dimension N .

From the plot of $\log(\Delta N)$ vs $\log(x)$ we estimate the critical exponent $\beta = 5$ (see Fig. 6).

The obtained dependence indicates transition from integrable phase labeled by I to chaotic one labeled by II at x_c . The critical density x_c depends on dimension N of the ensemble, therefore it would be interesting to investigate this dependence and to present the results in the form of the phase diagram Fig. 7. The diamonds on this diagram approximate the separatrix between the chaotic domain II and integrable one I. Domains I and II in the Figs 5, 7 represent systems having different physical properties. This is why we relate them to different phases. Therefore, presented analysis based on the concept of random matrices gives some information about the phase situation resulting from some general properties of Hamiltonian. These properties are more general than assumptions about the Hamiltonian forming renormalization group and the presented method allows to investigate also systems for which the Hamiltonian is unknowable.

The natural extension of the presented research is the Sparse Gaussian Complex Hermitian Random Ensemble — SGRHE($x_{\text{Re}}, x_{\text{Im}}, \mathcal{N}$), where \mathcal{N} is the dimension of the real matrices H_0, H_1 generating hermitian matrix H (compare [23], Table II), and x_{Re} is the fraction of the H_0 matrix elements not equal to zero, x_{Im} is the fraction of the H_1 matrix elements not equal to zero. The x_{Re} elements of matrix H_0 are zero-centred Gaussian distributed with variance equal to σ^2 , while the remaining elements are constant random variables equal identically to zero, distributed everywhere randomly (including the diagonal). The analogous situation holds for x_{Im} elements of H_1 . The elements are independent random variables. Among the other extensions there is the Sparse Gaussian Real Quaternion Self Dual Random Ensemble — SGRQSDE($x_0, x_1, x_2, x_3, \mathcal{N}$), where \mathcal{N} is the dimension of the real matrices H_0, H_1, H_2, H_3 generating real quaternion matrix H (compare [24], formulas (85), (89)), and x_μ is the fraction of the H_μ matrix elements not equal to zero, $\mu = 0, 1, 2, 3$. The x_μ elements of matrix H_μ are zero-centred Gaussian distributed with variance equal to σ^2 , while the remaining elements are constant random variables equal identically to zero, distributed everywhere randomly (including the diagonal). Analysis of the phase diagrams for SGRHE and SGRQSDE will extend our knowledge about the phase situation of quantum systems with broken symmetry from the unitary and symplectic ones. Expected results may shed some light onto explanation of the phenomena which are not completely understood yet, for instance HTS.

The authors are indebted to Prof. N.G. van Kampen for reading the manuscript and critical remarks.

REFERENCES

- [1] Y.V. Fyodorov, O.A. Chubykalo, F.M. Izrailev, G. Casati, *Phys. Rev. Lett.* **76**, 1603 (1996).
- [2] R.B. Griffiths, *Phys. Rev. Lett.* **23**, 17 (1969).
- [3] B.L. Altshuler, *J. Appl. Phys. Suppl.* **26**, 1938 (1987).
- [4] S. Kirkpatrick, T.P. Eggarter, *Phys. Rev.* **B 6**, 3598 (1972).
- [5] M.V. Berry, *Proc. Roy. Soc.* **A400**, 229 (1985).
- [6] G.J. Rodgers, C. De Dominicis, *J. Phys. A* **23**, 1567 (1990).
- [7] A.D. Mirlin, Y.V. Fyodorov, *J. Phys. A* **24**, 2273 (1991).
- [8] S.N. Evangelou, E.N. Economou, *Phys. Rev. Lett.* **68**, 361 (1992).
- [9] S.N. Evangelou, *J. Stat. Phys.* **69**, 361 (1992).
- [10] G.J. Rodgers, A.J. Bray, *Phys. Rev.* **B 37**, 3557 (1988).

- [11] E.P. Wigner, International Conference on the Neutron Interactions with the Nucleus (1957), Columbia University, New York, September 9–13, 1957, Columbia University Report No. CU-175 (TID-7547) (unpublished), p. 49.
- [12] E.P. Wigner, Conference on Neutron Physics by Time-of-Flight, (1957), Gatlinburg, Tennessee, November 1 and 2, 1956, Oak Ridge National Laboratory Report No. ORNL-2309 (unpublished), p.59.
- [13] C.E. Porter, *Statistical Theories of Spectra: Fluctuations*, Academic Press, New York 1965, p.223.
- [14] C.E. Porter, *Statistical Theories of Spectra: Fluctuations*, Academic Press, New York 1965, p. 199.
- [15] M.M. Duras, K. Sokalski, *Phys. Rev.* **E 54**, 3142 (1996).
- [16] L. Collatz, *Numerische Behandlung von Differentialgleichungen*, Springer-Verlag, Berlin, Goettingen, Heidelberg 1955, Appendix, Table II.
- [17] C.E. Porter, *Statistical Theories of Spectra: Fluctuations*, Academic Press, New York 1965, p. 6.
- [18] C.E. Porter, *Nucl. Phys.* **40**, 167 (1963).
- [19] P.B. Kahn, C.E. Porter, *Nucl. Phys.* **48**, 385 (1963).
- [20] L.E. Reichl, *The Transition to Chaos In Conservative Classical Systems: Quantum Manifestations*, Springer-Verlag, New York 1992, Chapter 6, p. 248.
- [21] F.J. Dyson, M.L. Mehta, *J. Math. Phys.* **4**, 713 (1963).
- [22] K. Sokalski, *Phys. Lett.* **A** (submitted).
- [23] C.E. Porter, *Statistical Theories of Spectra: Fluctuations*, Academic Press, New York 1965, p. 26.
- [24] C.E. Porter, *Statistical Theories of Spectra: Fluctuations*, Academic Press, New York 1965, p. 25.